Organic & Biomolecular Chemistry

Cite this: *Org. Biomol. Chem.*, 2011, **9**, 5436

www.rsc.org/obc

PAPER

A naphthalimide fluorophore with efficient intramolecular PET and ICT Processes: Application in molecular logic

Haixia Wang,[a,b] Haixia Wu,[a] Lin Xue,[a] Yan Shi[a] and Xiyou Li*[a]

Received 28th March 2011, Accepted 28th April 2011
DOI: 10.1039/c1ob05481c

A novel 4-amino-1,8-naphthalimide (NDI) with two different metal cation receptors connected at 4-amino or imide nitrogen positions respectively was designed and prepared. Significant internal charge transfer (ICT) as well as photoinduced electron transfer (PET) from the receptors to NDI is revealed by the shifted UV-vis absorption spectra and significant fluorescence quenching. Both Zn^{2+} and Cu^{2+} can coordinate selectively with the two cation receptors in this molecule with different affinities. The coordination of Zn^{2+} with the receptor at imide nitrogen hindered the PET process and accordingly restored the quenched fluorescence of NDI. But the coordination of Zn^{2+} at 4-amino position blocked the ICT process and caused significant blue-shift on the absorption peak with the fluorescence intensity unaffected. Similarly, coordination of Cu^{2+} with the receptor at imide nitrogen can block the PET process, but can not restore the quenched fluorescence of compound **3** due to the paramagnetic properties of Cu^{2+}, which quench the fluorescence significantly instead. With Cu^{2+} and Zn^{2+} as two chemical inputs and absorption or fluorescence as output, several logic gate operations, such as OR, NOR and INHIBIT, can be achieved.

Introduction

Molecular logic gates have attracted a lot of research interests since the first molecular AND logic gate had been reported by de Silva and co-workers[1] due to their potential applications in the creation of nanometre-scale molecular devices.[2] Numerous examples of the molecular logic gates are available in the literature which demonstrate AND,[3] OR,[4] NOT,[5] XOR,[6] INHIBIT,[7] NOR,[8] XNOR,[9] NAND[10] logic operations independently. With careful molecular design, the integration of distinctively different logic gate operations in one molecule is possible. A rational design is to decorate the molecule with multiple receptors and fluorophores, which can multiply the information input and output channels.[11] Combination of internal charge transfer (ICT) and photoinduced electron transfer process (PET) in one fluorophore has been proved to be an efficient way to increase output channels such as changes in absorption or emission spectra, which are the most common ones for the logic gate operations.[12] For logic gates with multiple inputs, high selectivity towards an outer stimulus is especially important. Metal ions, with their inherent selectivity for ligands, were a group of ideal candidates for chemical input and have been used in many molecular logic gates.[13] The abundant knowledge about the ligand–metal interactions allows one to propose exactly the selective interactions in a mixture of metal ions and different ligands, and thus the new molecules with prerequisite logic operations can be designed purposively.

In the present research, 4-amino-1,8-naphthalimide (NDI) was chosen as fluoroionophore, due to its remarkable optical properties, such as strong absorption and emission in the visible region, high fluorescence quantum yields, high photostability and large Stokes shift.[14] The amino group at the 4 position can play as an electron donor and cause strong ICT upon photo excitation. Therefore, interfering on the electron donating ability of amino group at the 4 position will cause significant changes to the absorption and emission peaks of this compound, which makes NDI compounds good candidates for the fluorophore of chemical sensors based on ICT process.[15] Moreover, NDIs are also good electron acceptors due to the strong electron-withdrawing properties of imide group. Once a receptor with good electron-donating properties is connected to NDI, PET can happen between receptor and fluorophore and thus a PET-based sensor can be designed.[16] NDI is therefore expected to be an ideal model to build a molecule with both ICT and PET processes and achieve integrated logic operations. However, related research is scarcely reported in literature.

Results and discussion

Molecular design and synthesis

We present a new NDI compound **3**, which has been selectively decorated with di(2-pyridylmethyl)amine (**DPA**) and N,N-di(2-pyridylmethyl)-*N′*-(*p*-aminophenyl)-ethylenediamine (**EDPA**) metal cation receptors at the 4-amino and imide positions,

[a]*Key laboratory of colloid and interface chemistry, Ministry of Education, Department of Chemistry, Shandong University, Jinan, China, 250100. E-mail: xiyouli@sdu.edu.cn; Fax: 86-531-88564464; Tel: 86-531-88369877*
[b]*Department of Chemistry, Henan Normal University, Xinxiang, China, 453007*

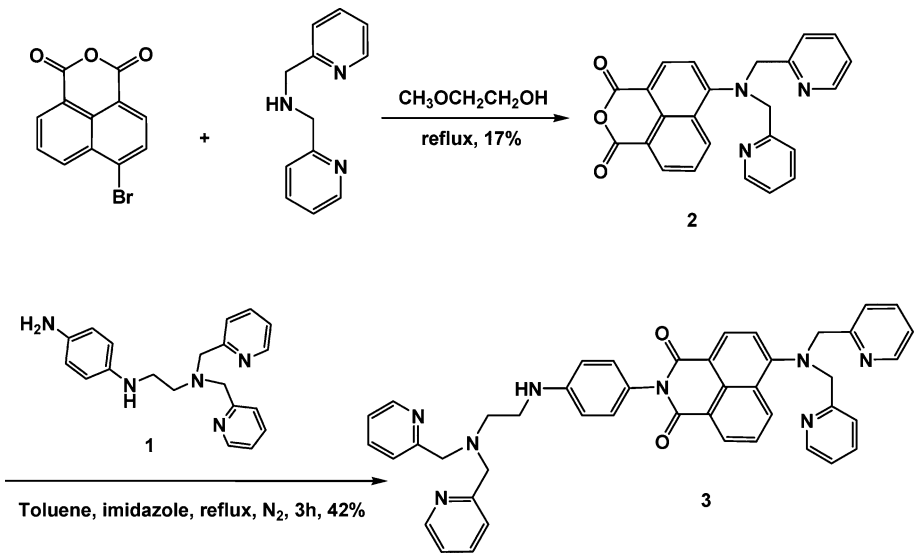

Scheme 1 Synthesis of compound **3**.

respectively. The structure and synthetic procedures are shown in Scheme 1. The coordination of metal ions with the DPA group at the 4 position is expected to affect the ICT from nitrogen to NDI efficiently and induce significant changes on the absorption and emission spectra.[15l] Meanwhile, the EDPA group at the imide nitrogen position is an electron donor, it can quench the fluorescence of NDI efficiently by a PET process. Coordination of metal ions at this position will reduce the electron-donating ability of EDPA and hinder the PET process, and then restore the fluorescence from NDI again. DPA and EDPA are expected to show different selectivity towards different metal ions as shown in our previous results.[17] Herein, with different metal ions as chemical inputs, and absorption and fluorescence spectra as outputs, this compound can perform multiple logic operations at molecular level.

Dipicolylamine is commercially available and reacts with 4-bromo-1,8-naphthalic anhydride in methyl glycol under reflux for 4 h to give compound **2**. Condensation of **2** with EDPA provides target compound **3** in reasonable yield. All products are purified repeatedly by column chromatograpahy on silica gel.

UV-vis absorption and emission spectra of 3 in the absence of different metal cations

Due to the electron-donating property of DPA at the 4 position and the electron-withdrawing property of the imide moiety, 4-amino-1,8-naphthalimide derivative **3** gives a "push–pull" based excited state. This ICT character gives rise to a broad absorption band in the visible region centered at about 410 nm ($\varepsilon = 12500\ M^{-1}\ cm^{-1}$), which is responsible for the yellow color of the solution in acetonitrile, and a broad emission band at about 520 nm in acetonitrile, respectively. On the other hand, the 4-amino-1,8-naphthalimide derivatives are usually found to be highly emissive in organic solvents. However, as expected compound **3** only demonstrates a low quantum yield of 10%. This indicates that the PET process from nitrogen atoms in the EDPA moiety to the fluorophore NDI happens with high efficiency and the excited state of naphthalimide is efficiently quenched by this PET process.

UV-vis absorption and emission spectra of 3 in the presence of different metal cations

Fig. 1 shows changes of absorption spectra of compound **3** upon addition of excess metal ions. The addition of metal ions, such as Mn^{2+}, Fe^{3+}, Hg^{2+}, Co^{2+}, Ni^{2+}, Cd^{2+}, Pb^{2+}, Cr^{3+} did not induce any significant changes on the absorption spectra. However, addition of Zn^{2+} produced a distinctive blue shift on the maximum absorption peak (from 406 to 358 nm). Similar changes on the absorption spectra were observed in the presence of Cu^{2+} with a blue shift on the maximum absorption peak as high as 82 nm. The changes of the absorption of **3** while adding Zn^{2+} or Cu^{2+} resulted in perceived color change from yellow to colorless to the naked eyes, as can be seen in the photograph. The significant changes on the absorption spectra indicate directly that compound **3** coordinates with Cu^{2+} and Zn^{2+} selectively. The changes on the absorbance of compound **3** at 406 nm after the addition of various metal ions are listed in Fig. 1b. It reveals clearly that compound **3** presents high selectivity towards Zn^{2+} and Cu^{2+} over other conventional metal ions.

Following the literature, receptor DPA normally shows high selectivity towards Cu^{2+}, Zn^{2+} and Cd^{2+} depending on the linkage and solvent.[18] The significant changes on the absorption spectra of compound **3** upon coordination of Zn^{2+} and Cu^{2+} revealed that the DPA linked at 4 position participated in the coordination with Zn^{2+} and Cu^{2+}. The distinctive blue-shift on the maximum absorption peak was caused by the reduced ICT process.

The fluorescence spectra of compound **3** in the presence of different metal cations are shown in Fig. 2a. The fluorescence intensities of compound **3** in the presence of different metal ions with same concentrations are shown in Fig. 2b. It can be found that free compound **3** shows a weak broad emission band with the peak maximum at about 519 nm and a fluorescence quantum yield of 10%. In the presence of Cu^{2+}, Ni^{2+}, Fe^{3+}, Cr^{3+} and Co^{2+}, the fluorescence of compound **3** was quenched completely. However, the addition of Hg^{2+}, Cd^{2+}, Pb^{2+} and Mn^{2+} induced about two times magnification on the fluorescence intensity without identical shift on peak wavelength. The most significant

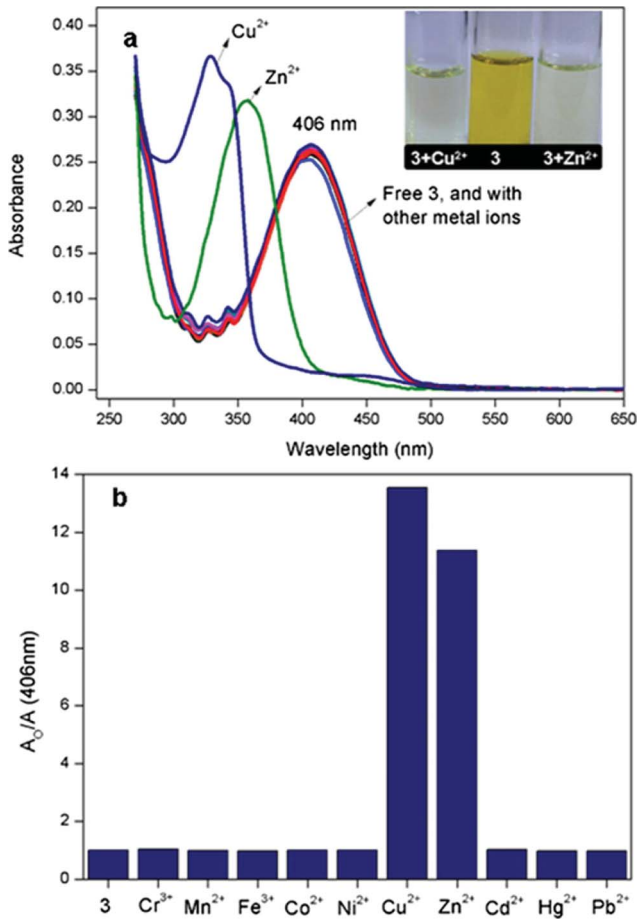

Fig. 1 (a) Absorption spectra of compound **3** (20 μM) in the presence of different metal cations (4 equiv. of **3**) in acetonitrile; (b) Absorption responses of compound **3** to various metal cations, A_0 represents the absorbance of free compound **3** at 406 nm while A represents the absorbance compound **3** in the presence of various metal ions.

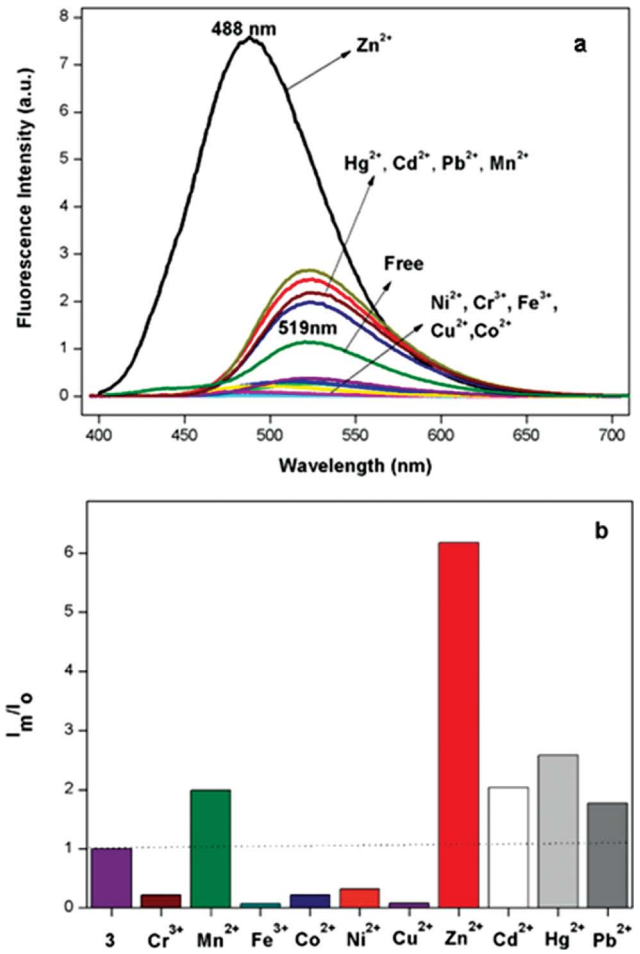

Fig. 2 (a) Fluorescence spectra of compound **3** (20 μM, λ_{ex} = 380 nm) in the presence of different metal cations (4 equiv. of **3**) in acetonitrile; (b) Emission responses of compound **3** (20 μM) to various metal cations (4 equiv. of **3**), I represents the integrated fluorescence intensity between 400 nm and 710 nm after it was normalized according to the absorbance at excitation wavelength. Subscripts m represents in the presence of metal cations and o represents lack of metal cations.

change on the fluorescence spectra was brought by Zn^{2+}, which induced a remarkable enhancement on the fluorescence quantum yield as well as a 50 nm blue-shift on the wavelength of band maximum.

As mentioned above, the low fluorescence quantum yield of compound **3** in solution resulted from the PET process. But the residue of the fluorescence suggests that the PET in compound **3** is not quick enough to quench all the fluorescence of compound **3**. The notable fluorescence quenching of compound **3** caused by the presence of Cu^{2+}, Ni^{2+}, Fe^{3+}, Cr^{3+} and Co^{2+} indicated that all these metal ions indeed coordinated with compound **3**. The paramagnetic properties of these metal ions induced non-radiative decay for the excited states of NDI and then causing the significant fluorescence quenching. The significant change on the absorption spectra of compound **3** revealed that Cu^{2+} was coordinated with the DPA group at the 4 position. But the coordination position of Ni^{2+}, Fe^{3+}, Cr^{3+} and Co^{2+} can not be determined at this stage because these metal ions will induce significant fluorescence quenching regardless of the coordination position. The moderate fluorescence enhancement of compound **3** caused by the presence of Hg^{2+}, Cd^{2+}, Pb^{2+} and Mn^{2+} could be attributed to the capture of these metal ions by the EDPA receptor at the imide nitrogen position, which hinders the PET process from EDPA to NDI and thus releases the quenched fluorescence of NDI by the PET process. We note that the enhanced fluorescence of compound **3** in the presence of these metal ions does not show significant shift on the peak maximum relative to that of free compound **3**, which indicates that the nitrogen atom at the 4 position of compound **3** did not participate in the coordination with these metal ions. The significant fluorescence enhancement of compound **3** caused by Zn^{2+} can also be attributed to the coordination of Zn^{2+} with EDPA at the imide nitrogen as that observed for Hg^{2+}, Cd^{2+}, Pb^{2+} and Mn^{2+}. The more significant fluorescence enhancement measured for Zn^{2+} than those of Hg^{2+}, Cd^{2+}, Pb^{2+} and Mn^{2+} may be attributed to the high affinity of EDPA towards Zn^{2+} over other metal ions as reported in the literature.[18p] The distinctive blue-shift on the maximum fluorescence peak of compound **3** in the presence of Zn^{2+} may result from the coordination of Zn^{2+} with PDA at the 4 position, too. The capture of Zn^{2+} by DPA that is conjugated to the NDI core resulted in a reduced ICT process, and this process magnified the energy gap between the HOMO and LUMO and thus caused the blue-shift on the fluorescence peak.

UV-vis absorption and emission spectra of 3 in the presence of different concentration of Zn^{2+}

In order to understand the coordination of compound **3** with Zn^{2+} in detail, the absorption spectra of compound **3** with different concentrations of Zn^{2+} were recorded as shown in Fig. 3. The changes on the absorption spectra of compound **3** along with the concentration increase of Zn^{2+} can be divided into two distinct stages. This is revealed clearly in Fig. 3b, which shows the plot of the absorbance of compound **3** at 409 nm against the concentration of Zn^{2+}. In the concentration range of 0–1.0 equiv. of Zn^{2+}, the absorption spectra of compound **3** had no significant change on both intensity and peak wavelength. However, when the concentration of Zn^{2+} in solution exceeded 1.0 equiv. of compound **3**, the absorbance at 409 nm decreased along with the increase of the Zn^{2+}concentration. Meanwhile, a new absorption peak at 358 nm formed, clearly suggesting the formation of a new compound in the solution.

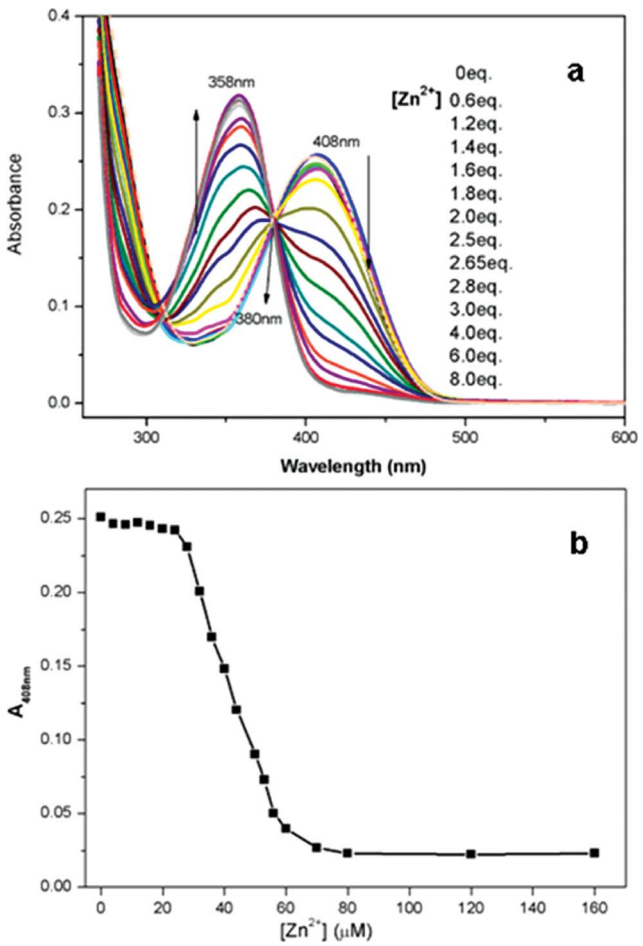

Fig. 3 (a) Absorption spectra of compound **3** in the presence of different concentration of Zn^{2+}; (b) Changes of the absorbance of compound **3** at 408 nm along with the concentration increase of Zn^{2+}.

The change of fluorescence spectra of compound **3** along with concentration increase of Zn^{2+} can also be divided distinctively into two stages as shown in Fig. 4. In the low concentration range of Zn^{2+} (0–1 equiv.), the emission peak of compound **3** at 518 nm increased dramatically in intensity without any detectable shift on the peak wavelength. However, in the range of higher concentration (>1 equiv.), further enhancement of the fluorescence intensity at 518 nm was not detected, but a slight blue-shift was observed. The plot of the fluorescence quantum yields of compound **3** against the concentration of Zn^{2+} reveals that the changes on the fluorescence spectra are synchronous with that of absorption spectra. We attributed the changes of the absorption and fluorescence spectra to the two step coordination of compound **3** with Zn^{2+}. For the first step, Zn^{2+} was coordinated to the EDPA group of compound **3** at the imide nitrogen position, the PET process was then hindered and the fluorescence of NDI was released. At the second step, Zn^{2+} began to bind with DPA at the 4 position, the ICT process was interrupted and the blue shift in the absorption and emission spectra was consequently observed. According to the Benesi–Hildebrand-type analysis, the stability constants of the complexes formed for the first and second step reaction were estimated to be 4.21×10^5 M^{-1} and 1.33×10^5 M^{-1} respectively.[17,19] The results indicate that the favorite position for Zn^{2+} to coordinate is the EDPA at imide nitrogen position.

The two step coordination of compound **3** with Zn^{2+} was further supported by the ^1H NMR titration experiments. Fig. 5 shows the ^1H NMR spectra of compound **3** in the presence of different concentration of Zn^{2+} and the assignment of the signals. It can be found that the signals of H_a, H_b, H_c, H_e and H_f shifted significantly when the concentration of Zn^{2+} increased from 0 to 1.0 equiv., which proved that Zn^{2+} was coordinated to EDPA at imide nitrogen position. While the content of Zn^{2+} in the solution exceeded 1 equiv. of compound **3**, the signals of the proton mentioned above did not shift anymore, but the signal of H_g shifted obviously instead, which indicated that Zn^{2+} began to coordinate with DPA. Further increase on the content of Zn^{2+} in the mixture did not induce further shifts on the signals of the protons but sharpened the signal peaks. This suggests that the formed coordination compounds between compound **3** and Zn^{2+} was stabilized by the presence of excess of Zn^{2+}.

The absorption and emission spectra of compound 3 in the presence of different concentration of Cu^{2+}

As mentioned above, the absorption and emission spectra of compound **3** showed remarkable changes upon the coordination of Cu^{2+}. In order to get more information on the coordination process between Cu^{2+} and compound **3**, the absorption spectra of compound **3** in the presence of different concentrations of Cu^{2+} were also recorded. The results are shown in Fig. 6a. Similar to the results observed for the coordination of Zn^{2+}, the absorption spectra of compound **3** had no significant changes when the content of Cu^{2+} in the solution was less than 1.0 equiv. Further increase on the concentration of Cu^{2+} in the solution, the absorbance of **3** at 406 nm gradually decreased following the formation of a new band centered at 328 nm, and an isobestic point at 356 nm was clearly observed. Upon addition of 3.5 equiv. of Cu^{2+}, the peak at 406 nm disappeared completely. The experiment results mean that the coordination of compound **3** with Cu^{2+} in acetonitrile could also be divided into two stages like Zn^{2+}, as can be seen in Fig. 6b. In the concentration range of 0–1.0 equiv. of Cu^{2+}, the absorption spectra of compound **3** had no significant changes on both intensity and peak wavelength, which indicates that Cu^{2+} is coordinated to DPA at the 4 position. Further

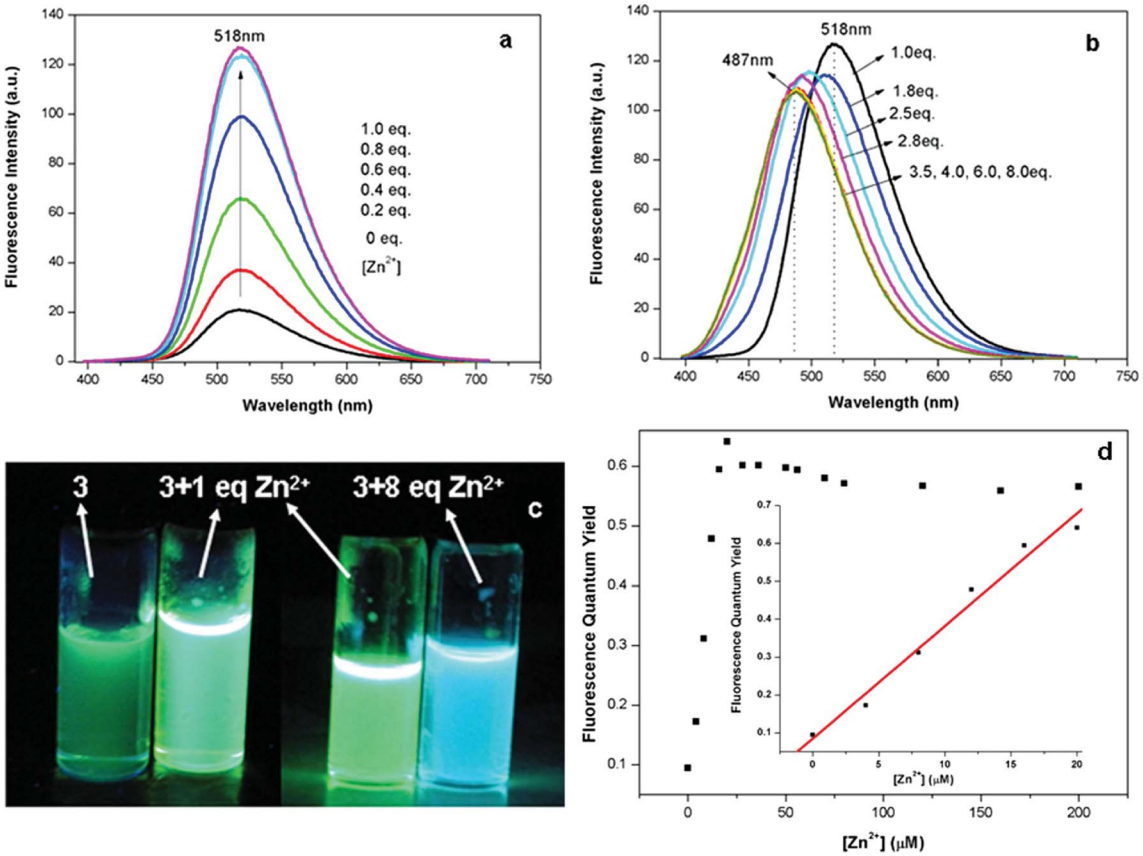

Fig. 4 Emission spectra of compound **3** (20 μM, λ_{ex} = 380 nm) in the presence of Zn^{2+} in acetonitrile solution. (a) The concentration range of Zn^{2+} is 0, to 1.0; (b) The concentration range of Zn^{2+} is 1.0 to 8.0; (c) Photograph of compound **3** (4.5×10^{-3} M) in the presence of different concentration of Zn^{2+} in acetonitrile under UV light; (d) The change of fluorescence quantum yield of compound **3** along with the increasing on Zn^{2+} concentrations in acetonitrile; The inset profile represents the change of fluorescence quantum yield with the concentration of zinc ions in the range of 0-20 μM.

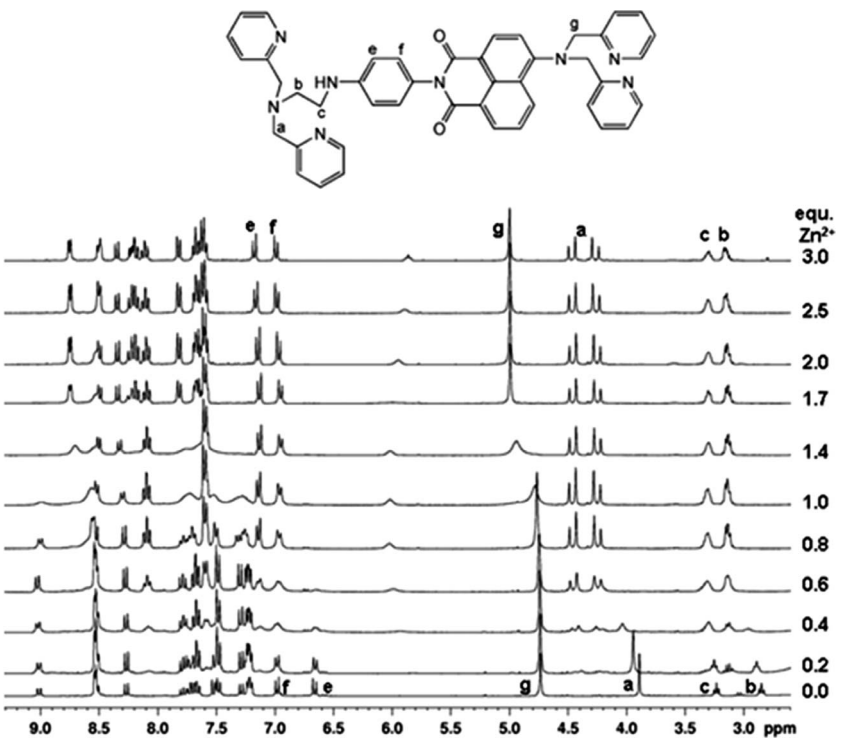

Fig. 5 ^{1}H NMR spectra of compound **3** in CD_3CN in the presence of various concentration of Zn^{2+}.

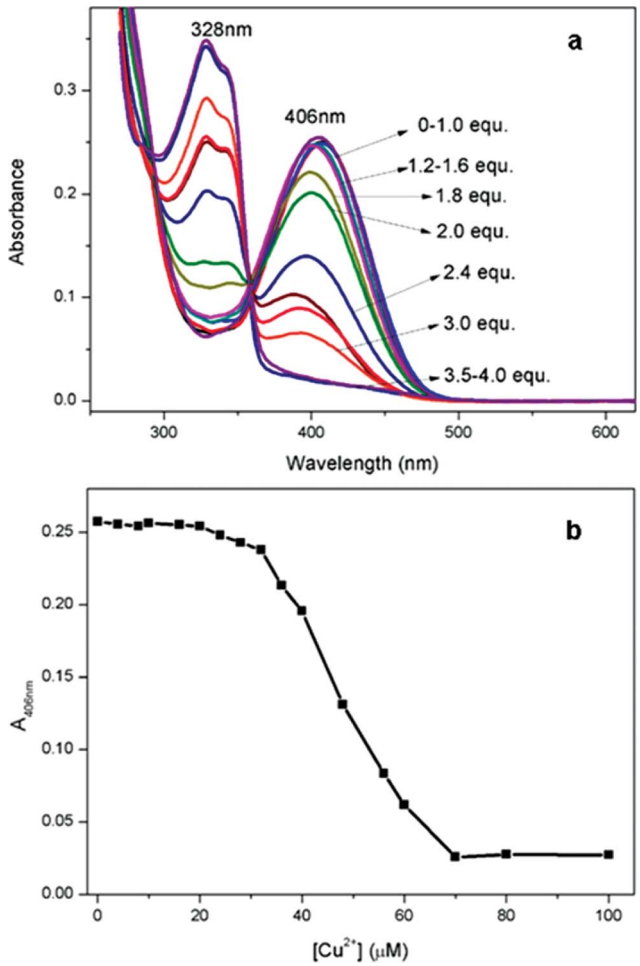

Fig. 6 (a) Absorption spectra of compound **3** (20 μM) in acetonitrile in the presence of various concentrations of Cu^{2+}; (b) Changes of the absorbance of compound **3** at 406 nm as a function of Cu^{2+} concentration.

addition of Cu^{2+} in the solution gave rise to a large blue-shift on the absorption maximum and a clear isobestic point at 356 nm, which reveals that Cu^{2+} is coordinated to DPA at the 4 position at this concentration range.

The fluorescence spectra of compound **3** with different concentrations of Cu^{2+} are shown in Fig. 7. Unlike Zn^{2+}, the addition of Cu^{2+} induced significant fluorescence quenching, which accompanied an obvious blue-shift on the maximum emission peak. In combination with the results of absorption experiments, we speculate that Cu^{2+} could bind with both EDPA and DPA of compound **3**, but the complex formed with EDPA has higher stability. Therefore, in the low concentration rang of Cu^{2+}, EDPA binds with most of the Cu^{2+} in solution. That is why the UV-vis absorption spectra did not show significant change at this stage. Because of the paramagnetic nature of Cu^{2+}, the coordination of Cu^{2+} at EDPA position will also introduce massive no-radiative decay for the excited states of NDI. Two controversial processes are now operating on the fluorescence intensity of compound **3**. On the one hand, the fluorescence of compound **3** is quenched by the presence of paramagnetic Cu^{2+}, on the other hand, the fluorescence of NDI is enhanced by the hindered PET process between EDPA and NDI due to the coordination of Cu^{2+}. The fluorescence intensity decreased in the low concentration range

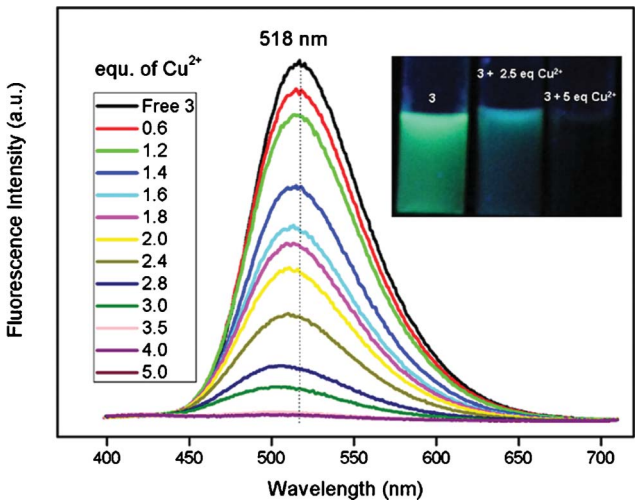

Fig. 7 Emission spectra of compound **3** (20 μM) in the presence of various concentrations of Cu^{2+}, and photograph of **3** in the presence of different concentration of Cu^{2+} in acetonitrile under UV light.

of Cu^{2+} as shown in Fig. 7, which indicates that the fluorescence quenching caused by the paramagnetic property of Cu^{2+} dominates the process. In the higher concentration range of Cu^{2+}, DPA at the 4 position conjugating to the NDI core begins to participate in the coordination with Cu^{2+}, and accordingly the fluorescence is efficiently quenched with the maximum emission peak blue-shifted simultaneously as that reported in literature.[18o]

Competition coordination between Cu^{2+} and Zn^{2+}

Fig. 8a shows the absorption spectra of compound **3** with 3 equiv. of Zn^{2+} and various concentrations of Cu^{2+}. The absorption spectrum of compound **3** in the presence of 3 equiv. of Zn^{2+} produced a maximum absorption at 359 nm, which blue-shifted for about 50 nm relative to that of pure compound **3** and can be assigned to the coordination of Zn^{2+} with DPA at the 4 position. The addition of a small amount of Cu^{2+}, such as 0.6 equiv., induced a mild blue shift on the absorption spectra, but with further increase on the amount of Cu^{2+} in the solution, the absorption peak at 359 nm decreased gradually, which coincided with the growing of a new peak at 328 nm. This change can be ascribed to the complex of DPA at the 4 position of compound **3** with Cu^{2+}. When the amount of Cu^{2+} increased to 4 equiv. of compound **3**, the absorption spectra grew into typical absorption spectra of compound **3** in the presence of pure Cu^{2+}. This result indicates that the Zn–DPA complex has completely transferred into Cu–DPA complex, suggesting that DPA at the 4 position prefers to chelate Cu^{2+} instead of Zn^{2+}. The fluorescence spectra of compound **3** in the presence of both Zn^{2+} and Cu^{2+} are shown in Fig. 8b. Addition of 3 equiv. of Zn^{2+} showed a maximum emission band at about 492 nm, which blue-shifted for about 30 nm relative to that of free compound **3**, and significant fluorescence quenching. When the amount of Cu^{2+} in the mixture increased to 4 equiv. of compound **3**, the fluorescence was completely quenched. This result suggests that the coordination of DPA at the 4 position with Zn^{2+} has been completely edged out by the coordination with Cu^{2+}, which corresponds well with the results of absorption spectra.

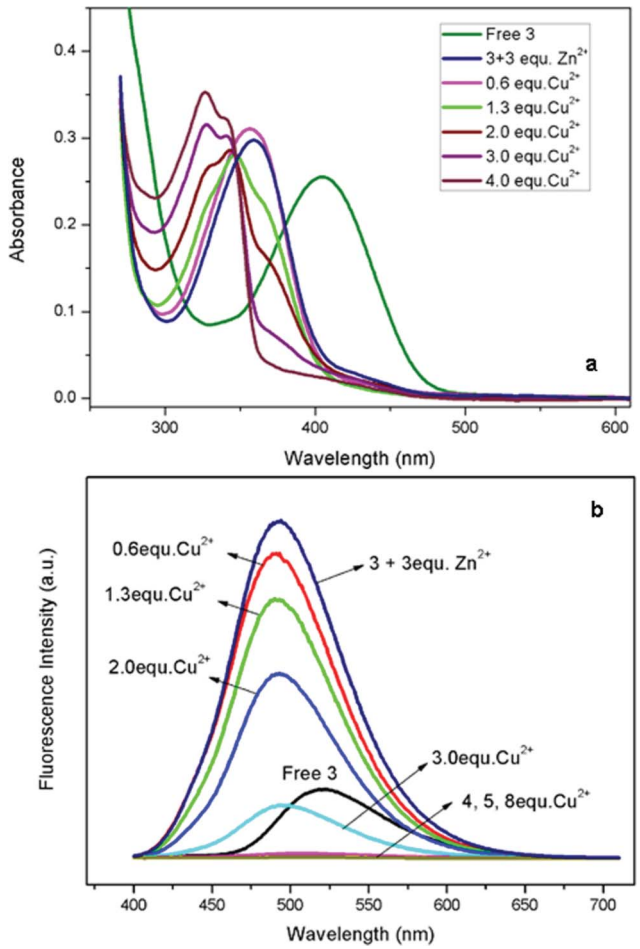

Fig. 8 Absorption(a) and fluorescence (b) spectra of compound **3** (20 μM) in the presence of 3 equiv. of Zn^{2+} and various concentration of Cu^{2+} in acetonitrile. (λ_{ex} = 380 nm).

Logic operations based on the absorption and fluorescence spectra of compound 3

It is well known that one can design a single molecule which can simultaneously behave as two (or more) distinct logic gates, depending on the exact choice or definition of outputs.[12a] Take the advantage of high selectivity of compound **3** towards Zn^{2+} and Cu^{2+}, different logic operations with Zn^{2+} and Cu^{2+} as two chemical inputs and absorption or emission spectra as multiple channel outputs may be achieved. Fig. 9 (Top) compares the absorption spectra of free compound **3**, **3** + 3 equiv. Zn^{2+}, **3** + 3 equiv. Cu^{2+} and **3** + 3 equiv. Cu^{2+} + 3 equiv. Zn^{2+}. With the absorbance at 350 nm as the output signal, the absorbance of free compound **3** (no chemical input) is small (0.07 a.u.). But in the presence of Zn^{2+} or Cu^{2+} or both Zn^{2+} and Cu^{2+}, the absorbance at this point increased to 0.26 a.u.. This observations are correlated with a two input OR logic gate. The truth table is shown in Fig. 9 (Bottom). If we choose the absorbance at 405 nm as the output signal, the NOR logic operation can be achieved. Without any chemical input, the absorbance at 405 nm is high, but in the presence of either Zn^{2+}, or Cu^{2+}, the output signal is small. Similar small output signal is also observed in the presence of both Zn^{2+} and Cu^{2+}.

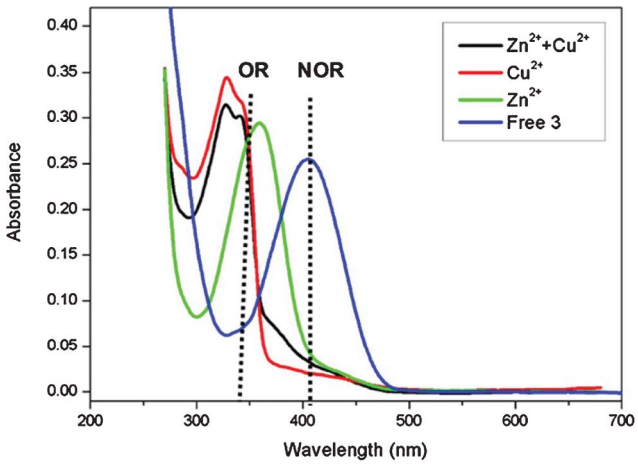

Input 1 Zn^{2+}	Input 2 Cu^{2+}	Output 1 **OR** A_{348nm}	Output 2 **NOR** A_{405nm}
0	0	0	1
1	0	1	0
0	1	1	0
1	1	1	0

Fig. 9 Top: Absorption spectra of compound **3**, **3** + 3 equiv. Zn^{2+}, **3** + 3 equiv. Cu^{2+} and **3** + 3 equiv. Zn^{2+} + 3 equiv. Cu^{2+}. Bottom: The truth table for the OR/NOR logic gates (Positive logic; 0: low signal, 1: high signal).

The fluorescence spectra of compound **3** in the presence of Zn^{2+}or Cu^{2+} and both of them are shown in Fig. 10. Without any chemical input, free compound **3** did not show any strong emission at 492 nm. But in the presence of Zn^{2+}, the intensity of the fluorescence at 492 nm increased significantly. On the contrary, the presence of Cu^{2+} quenched the fluorescence of compound **3** at 492 nm. In the presence of both Zn^{2+} and Cu^{2+}, compound **3** presents fluorescence again but with small intensity. With the fluorescence quantum yields as output signals and 0.25 is defined at the gate limit. The fluorescence quantum yield of compound **3** in the presence of Zn^{2+} is larger than 0.25 and therefore the output is 1, but in the presence of Cu^{2+}, both of Cu^{2+} and Zn^{2+}, as well as free compound **3**, the fluorescence quantum yields are all smaller than 0.25 and the output is 0. The fluorescence intensity changes described above mimic the function of an INHIBIT logic gate. The truth table and logic diagram are shown in Fig. 11.

Conclusion

From a view of a potential application, the reset capability is very important for the chemical-driven logic operations. Although various reset strategies have been addressed in some molecular systems, the low reset capabilities are all the same main drawbacks of molecular logic gates with chemical inputs. But the potential application of molecular based logic gates in a small space such as the inside of a cell makes the research on this topic still prospective.[12a] In the present research, we have designed and prepared successfully a new compound based on naphthalic imide, which bears both intramolecular ICT and PET processes. Selective coordination of Zn^{2+} and/or Cu^{2+} with this compound at different positions can block selectively the above mentioned

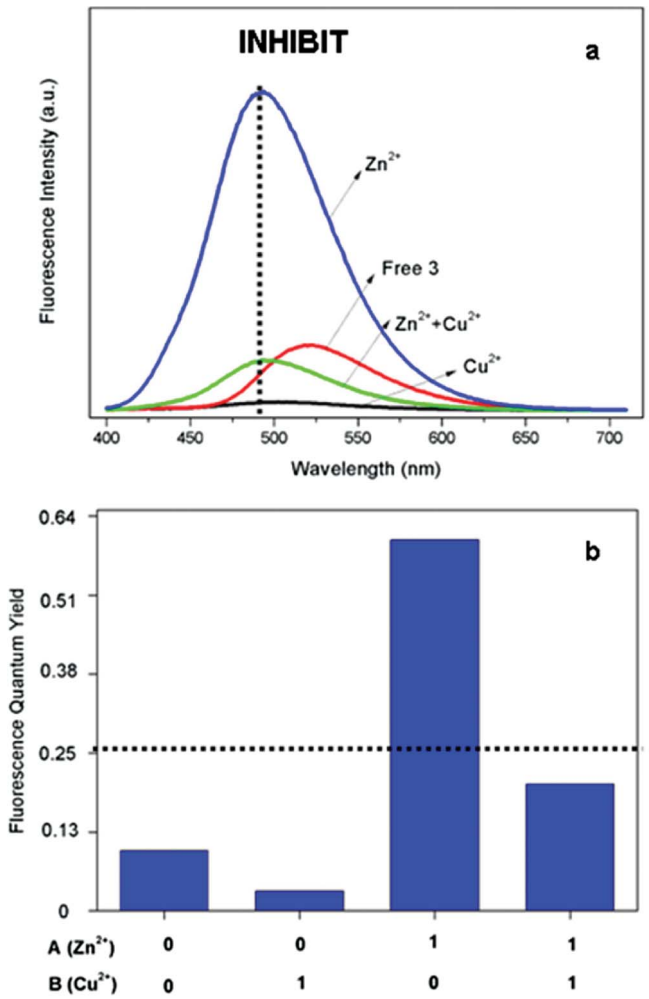

Fig. 10 (a) Fluorescence spectra of compound **3**, **3** with 3 equiv. Zn^{2+}, **3** with 3 equiv. Cu^{2+}, and **3** with 3 equiv. Zn^{2+} + 3 equiv. Cu^{2+}. The concentration of **3** was 20 μM; (b) The corresponding fluorescence quantum yield of compound **3** under different conditions.

Input 1 Zn^{2+}	Input 2 Cu^{2+}	Output INH I_{492nm}
0	0	0
1	0	1
0	1	0
1	1	0

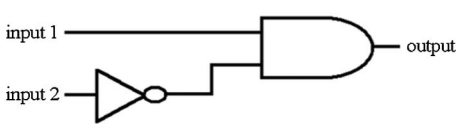

Fig. 11 The truth table for the INHIBIT logic gate and the corresponding logic diagram (Positive logic; 0: low signal, 1: high signal).

intramolecular process. The responses of the molecule towards outer stimulus are therefore enriched and thus the sensing of multiple species by one sensor with high selectivity can be achieved. More importantly, the newly designed molecule could perform NOR, OR and INH logic operations simultaneously with Zn^{2+} and Cu^{2+} as chemical inputs and absorption or emission spectra as outputs. These results will be useful for further molecular design to mimic the function of complex logic gates. Due to versatile structural modification on naphthalene imides, more complicated logic operations will be constructed. Related research is being carried out on in our lab.

Experimental section

General methods

^{1}H and ^{13}C NMR spectra were recorded on a Bruker 300 MHz NMR spectrometer with chemical shifts reported in ppm (in $CDCl_3$, TMS as internal standard). Mass spectra were recorded on a LCQ advantage spectrometer with ESI resource. HRMS were recorded on APEXII and ZAB-HS spectrometers. UV-vis absorption spectra were measured on HITACHI U-4100 spectrophotometer. Fluorescence emission spectra were recorded on an ISS K2 system.

Materials

The salts used in stock solutions of metal ions were $CrCl_3{\cdot}6H_2O$, $MnCl_2{\cdot}4H_2O$, $FeCl_3{\cdot}6H_2O$, $CoCl_2{\cdot}6H_2O$, $NiCl_2{\cdot}6H_2O$, $CuCl_2{\cdot}6H_2O$, $Zn(NO_3)_2{\cdot}6H_2O$, $CdCl_2{\cdot}2.5H_2O$, $Hg(NO_3)_2$, $Pb(NO_3)_2$. *N*-(4-Amino-phenyl)-*N*′,*N*′-di(2-picolyl) ethylene diamine was synthesized according to literature methods.[15f,17] Other chemicals were purchased from commercial sources. Solvents were of analytical grade and purified by standard methods.

4-*N*-di(2′-pyridylmethyl)amino-1,8-naphthalic anhydride (2). In a 100 ml round bottom flask, di(2-pyridylmethyl)amine (430 mg, 2.15 mmol) and monomethylglycol ether (50 ml) was added. The mixture was stirred at room temperature for 5 min. Then 4-bromo-1,8-naphthalic anhydride (500 mg, 1.8 mmol) was added to the flask. After the reaction mixture was refluxed at 125 °C for 4 h it was cooled to room temperature and diluted with 10 ml CH_2Cl_2. The organic layer was washed with water (3 × 80 ml) to remove the water soluble solvents and dried over $MgSO_4$ overnight. CH_2Cl_2 was removed under reduced pressure. The residue was purified by column chromatography on silica with $CH_3OH/CHCl_3$ (v/v) as eluent. The product was collected as a pale yellow solid (120 mg, 0.30 mmol) with a yield of 17%. mp >250 °C; ^{1}H NMR (300 MHz, $CDCl_3$, 25 °C, TMS): δ = 9.00 (d, J = 8.3 Hz, 1H, naphthyl), 8.60 (m, 3H, naphthyl + pyridyl), 8.38 (d, J = 8.4 Hz, 1H, naphthyl), 7.73 (t, J = 8.1 Hz, 1H, naphthyl), 7.64 (d, J = 7.8 Hz, 2H, pyridyl), 7.37 (d, J = 7.8 Hz, 2H, pyridyl), 7.26 (m, 3H, pyridyl + naphthyl), 4.80 (s, 4H, NCH_2); MS (ESI): m/z: 396.13 [M+H$^+$]; Calcd for $C_{24}H_{18}N_3O_3$: 396.42. High resolution MS (ESI): m/z: 396.1250 (M+H$^+$); Calcd for $C_{24}H_{18}N_3O_3$: 396.1248.

***N*-*p*-(*N*′-2-(*N*′,*N*′-di(2-pyridylmethyl)amino-ethylene)aniline)-4-*N*″-di(2-pyridylmethyl) amino-1,8-naphthalimide (3).** *N*-(4-amino-phenyl)-*N*′,*N*′-di-(2-picolyl) ethylene diamine (185 mg, 0.56 mmol) was added to a mixture of 20 ml dried toluene and 2 g imidazole. Under the protection of nitrogen, 4-*N*-di(2′-pyridylmethyl)amino-1,8-naphthyl anhydride (**2**) (110 mg, 0.27 mmol) was added to the mixture. After refluxing at 110 °C for 3 h,

the reaction mixture was diluted with 100 ml CH_2Cl_2 and washed with water to remove imidazole. The organic layer was dried over $MgSO_4$ for overnight and the solvents were removed under reduced pressure. The residue was purified by column chromatography on silica gel with CH_3OH/CH_2Cl_2 as eluent. The product was collected as yellow oil (82 mg, 0.11 mmol) with a yield of 42%. mp >250 °C; UV-vis, λ_{max} 406 nm ($\varepsilon = 1.25 \times 10^4$ mol L^{-1} cm^{-1}); ^1H NMR (300 MHz, $CDCl_3$, 25 °C, TMS): $\delta = 8.94$ (d, $J = 8.3$ Hz, 1H, naphthyl), 8.62 (m, 5H, naphthyl + pyridyl), 8.41 (d, $J = 8.1$ Hz, 1H, naphthyl), 7.76–7.57 (m, 5H, naphthyl + pyridyl), 7.47 (d, $J = 7.8$ Hz, 2H, pyridyl), 7.39 (d, $J = 7.8$ Hz, 2H, pyridyl), 7.18 (m, 5H, naphthyl + pyridyl), 7.03 (d, $J = 8.4$ Hz, 2H, phenyl), 6.68 (d, $J = 8.4$ Hz, 2H, phenyl), 4.76 (s, 4H; NCH_2), 3.94(s, 4H, NCH_2), 3.24 (t, $J = 5.4$ Hz, 2H, NCH_2), 2.95(t, $J = 5.4$ Hz, 2H, CH_2); ^{13}C NMR (300 MHz, $CDCl_3$, 25 °C, TMS): $\delta = 165.0$, 164.5, 157.3, 153.7, 149.6, 148.4, 136.7, 136.6, 132.3, 131.4, 130.5, 129.0, 126.8, 125.9, 124.4, 123.7, 123.3, 122.5, 122.3, 117.7, 116.9, 113.0, 60.2, 59.9, 52.6, 41.2; MS(ESI) *m/z*: 711.42 [M+H$^+$], Calcd for $C_{44}H_{38}N_8O_2$: 711.31.

Acknowledgements

Financial support from the Natural Science Foundation of China (Grant No. 21073112, 20771066) and instrument support from Key lab of Photochemical Conversion and Optoelectronic Materials of Chinese Academy of Science are gratefully acknowledged.

References

1 A. P. de Silva, H. Q. N. Gunaratne and C. P. McCoy, *Nature*, 1993, **364**, 42.
2 (*a*) F. M. Raymo, *Adv. Mater.*, 2002, **14**, 401; (*b*) A. P. de Silva and N. D. McClenaghan, *Chem.–Eur. J.*, 2004, **10**, 574; (*c*) P. Ball, *Nature*, 2000, **406**, 118–120; (*d*) V. Balzani, M. Venturi and A. Credi, *Molecular Devices and Machines: A Journey into the Nanoworld*, Wiley-VCH, Weinheim, Germany, 2003; (*e*) A. P. de Silva and S. Uchiyama, *Nat. Nanotechnol.*, 2007, **2**, 399; (*f*) D. C. Magri, T. P. Vance and A. P. de Silva, *Inorg. Chim. Acta*, 2007, **360**, 751; (*g*) A. Credi, *Angew. Chem., Int. Ed.*, 2007, **46**, 5472.
3 (*a*) A. P. de Silva, H. Q. N. Gunaratne and C. P. McCoy, *J. Am. Chem. Soc.*, 1997, **119**, 7891; (*b*) H. Wang, D. Zhang, X. Guo, L. Zhu, Z. Shuai and D. Zhu, *Chem. Commun.*, 2004, 670; (*c*) Z. Zhao, Y. Xing, Z. Wang and P. Lu, *Org. Lett.*, 2007, **9**, 547.
4 (*a*) P. Ghosh, P. K. Bharadwaj, S. Mandal and S. Ghosh, *J. Am. Chem. Soc.*, 1996, **118**, 1553; (*b*) N. J. Youn and S.-K. Chang, *Tetrahedron Lett.*, 2005, **46**, 125.
5 (*a*) A. P. de Sliva, S. A. de Sliva, A. S. Dissanayake and K. R. A. S. Sandanayake, *J. Chem. Soc., Chem. Commun.*, 1989, **1054**; (*b*) A. P. de Silva, H. Q. N. Gunaratne and P. L. M. Lynch, *J. Chem. Soc., Perkin Trans. 2*, 1995, 685; (*c*) M. N. Stojanovic, T. E. Mitchell and D. Stefanovic, *J. Am. Chem. Soc.*, 2002, **124**, 3555; (*d*) T. Gunnlaugsson, A. P. Davis and M. Glynn, *Chem. Commun.*, 2001, 2556.
6 (*a*) A. P. de Silva and N. D. McClenaghan, *J. Am. Chem. Soc.*, 2000, **122**, 3965; (*b*) A. Credi, V. Balzani, S. J. Langford and J. F. Stoddart, *J. Am. Chem. Soc.*, 1997, **119**, 2679.
7 (*a*) T. Gunnlaugsson, D. A. MacDonaill and D. Parker, *Chem. Commun.*, 2000, 93; (*b*) D. H. Qu, F. Y. Ji, Q. C. Wang and H. Tian, *Adv. Mater.*, 2006, **18**, 2035; (*c*) T. Gunnlaugsson, D. A. MacDonaill and D. Parker, *J. Am. Chem. Soc.*, 2001, **123**, 12866; (*d*) M. Kluciar, R. Ferreira, B. de Castro and U. Pischel, *J. Org. Chem.*, 2008, **73**, 6079.
8 (*a*) A. P. de Silva, I. M. Dixon, H. Q. N. Gunaratne, T. Gunnlaugsson, P. R. S. Maxwell and T. E. Rice, *J. Am. Chem. Soc.*, 1999, **121**, 1393; (*b*) Z. Wang, G. Zheng and P. Lu, *Org. Lett.*, 2005, **7**, 3669; (*c*) P. N. Cheng, P. T. Chiang and S. H. Chiu, *Chem. Commun.*, 2005, 1285.
9 (*a*) M. Asakawa, P. R. Ashton, V. Balzani, A. Credi, G. Mattersteig, O. A. Matthews, M. Montalti, N. Spencer, J. F. Stoddart and M. Venturi, *Chem.–Eur. J.*, 1997, **3**, 1992; (*b*) S. H. Lee, J. Y. Kim, S. K. Kim, J. H. Lee and J. S. Kim, *Tetrahedron*, 2004, **60**, 5171.
10 (*a*) S. Iwata and K. Tanaka, *J. Chem. Soc., Chem. Comm.*, **1995**, 1491; (*b*) O. S. Wolfbeis and H. Offenbacher, *Monatsh. Chem.*, 1984, **115**, 647; (*c*) M. W. Hosseini, A. J. Blacker and J.-M. Lehn, *J. Am. Chem. Soc.*, 1990, **112**, 3896; (*d*) D. Parker and J. A. G. Williams, *Chem. Commun.*, 1998, 245.
11 A. P. de Silva, N. D. McClenaghan and C. P. McCoy, *Molecular Switches*, Wiley-VCH, Weinheim, Germany, 2001.
12 (*a*) O. A. Bozdemir, R. Guliyev, O. Buyukcakir, S. Selcuk, S. Kolemen, G. Gulseren, T. Nalbantoglu, H. Boyaci and E. U. Akkaya, *J. Am. Chem. Soc.*, 2010, **132**, 8029; (*b*) A. Coskun, E. Deniz and E. U. Akkaya, *Org. Lett.*, 2005, **7**, 5187; (*c*) A. P. de Silva and N. D. McClenaghan, *Chem.–Eur. J.*, 2002, **8**, 4935.
13 (*a*) X. Zhao and C. Z. Huang, *Analyst*, 2010, **135**, 2853; (*b*) B. Valeur and I. Leray, *Coord. Chem. Rev.*, 2000, **205**, 3; (*c*) J. P. Desvergne and A. W. Czarnik, *Chemosensors of Ion and Molecule Recognition*, Kluwer Academic, Dordrecht, Netherlands, 1997.
14 (*a*) E. Martin, J. L. G. Coronado and J. J. Cammacho, *J. Photochem. Photobiol., A*, 2005, **175**, 1; (*b*) Y. Gao and R. A. Marcus, *J. Phys. Chem. A*, 2002, **106**, 1956; (*c*) J. Gan, Q. Song, X. Hou, K. Chen and H. Tian, *J. Photochem. Photobiol., A*, 2004, **162**, 399; (*d*) D. Kolosov, V. Adamovich, P. Djurovich, M. E. Thompson and C. Adachi, *J. Am. Chem. Soc.*, 2002, **124**, 9945; (*e*) R. M. Duke, E. B. Veale, F. M. Pfeffer, P. E. Kruger and T. Gunnlaugsson, *Chem. Soc. Rev.*, 2010, **39**, 3936; (*f*) X. Qian, Y. Xiao,Y. Xu, X. Guo, J. Qiana and W. Zhua, *Chem. Commun.*, 2010, **46**, 6418.
15 (*a*) D. Staneva, I. Grabchev, J. Soumillion and V. Bojinov, *J. Photochem. Photobiol., A*, 2007, **189**, 192; (*b*) V. B. Bojinov and T. N. Konstantinova, *Sens. Actuators, B*, 2007, **123**, 869; (*c*) H. He, M. A. Mortellaro, M. J. P. Leiner, S. T. Young, R. J. Fraatz and J. K. Tusa, *Anal. Chem.*, 2003, **75**, 549; (*d*) X. Guo, X. Qian and L. Jia, *J. Am. Chem. Soc.*, 2004, **126**, 2272; (*e*) Z. Xu, Y. Xiao, X. Qian, J. Cui and D. Cui, *Org. Lett.*, 2005, **7**, 889; (*f*) J. Wang, Y. Xiao, Z. Zhang, X. Qian, Y. Yang and Q. Xu, *J. Mater. Chem.*, 2005, **15**, 2836; (*g*) Z. Xu, X. Qian, J. Cuia and R. Zhang, *Tetrahedron*, 2006, **62**, 10117; (*h*) T. Gunnlaugsson, P. E. Kruger, T. C. Lee, R. Parkesh, F. M. Pfeffera and G. M. Husseya, *Tetrahedron Lett.*, 2003, **44**, 6575; (*i*) T. Gunnlaugsson, P. E. Kruger, T. C. Lee, R. Parkesh, F. M. Pfeffera and G. M. Husseya, *Tetrahedron Lett.*, 2003, **44**, 8909; (*j*) H. Ali and G. M. Hussey, *J. Org. Chem.*, 2005, **70**, 10875; (*k*) D. Cui, X. Qian, F. Liu and R. Zhang, *Org. Lett.*, 2004, **6**, 2757; (*l*) Z. Xu, X. Qian and J. Cui, *Org. Lett.*, 2005, **7**, 3029.
16 J. Wang and X. Qian, *Chem. Commun.*, 2006, 109.
17 H. Wang, D. Wang, Q. Wang, X. Li and C. A. Schalley, *Org. Biomol. Chem.*, 2010, **8**, 1017.
18 (*a*) H.-W. Rhee, C.-R. Lee, S.-H. Cho, M.-R. Song, M. Cashel, H. E. Choy, Y.-J. Seok and J.-I. Hong, *J. Am. Chem. Soc.*, 2008, **130**, 784; (*b*) H. M. Kim, M. S. Seo, M. J. An and B. R. Cho, *Angew. Chem.*, 2008, **120**, 5245; (*c*) X. Peng, J. Du, J. Fan, J. Wang, Y. Wu and J. Zhao, *J. Am. Chem. Soc.*, 2007, **129**, 1500; (*d*) K. Komatsu, K. Kikuchi, H. Kojima, Y. Urano and T. Nagano, *J. Am. Chem. Soc.*, 2005, **127**, 10197; (*e*) A. Ojida, Y. Mito-oka, K. Sada and I. Hamachi, *J. Am. Chem. Soc.*, 2004, **126**, 2454; (*f*) T. Hirano, K. Kikuchi, Y. Urano and T. Nagano, *J. Am. Chem. Soc.*, 2002, **124**, 6555; (*g*) S. C. Burdette, G. K. Walkup, B. Spingler, R. Y. Tsien and S. J. Lippard, *J. Am. Chem. Soc.*, 2001, **123**, 7831; (*h*) T. Hirano, K. Kikuchi, Y. Urano and T. Higuchi, *J. Am. Chem. Soc.*, 2000, **122**, 12399; (*i*) Z. Liu, C. Zhang, Y. Li, Z. Wu, F. Qian, X. Yang, W. He, X. Gao and Z. Guo, *Org. Lett.*, 2009, **11**, 795; (*j*) E. Ballesteros, D. Moreno, T. Gómez, T. Rodríguez, J. Rojo, M. García-Valverde and T. Torroba, *Org. Lett.*, 2009, **11**, 1269; (*k*) S. Atilgan, T. Ozdemir and E. U. Akkaya, *Org. Lett.*, 2008, **10**, 4065; (*l*) J. D. Amilan, M. Sandhya and G. Amrita, *Org. Lett.*, 2007, **9**, 1979; (*m*) X. Zhang, K. S. Lovejoy, A. Jasanoff and S. J. Lippard, *Proc. Natl. Acad. Sci. U. S. A.*, 2007, **104**, 10780; (*n*) S. A. de Silva, A. Zavaleta, D. E. Baron, O. A. Edward, V. Isidor, N. Kashimura and J. M. Percarpio, *Tetrahedron Lett.*, 1997, **38**, 2237; (*o*) S. Banthia and A. Samanta, *New J. Chem.*, 2005, **29**, 1001; (*p*) R. Trokowski, J. Ren, F. K. Kalman and A. D. Sherry, *Angew. Chem., Int. Ed.*, 2005, **44**, 6920.
19 (*a*) Y. Shiraishi, S. Sumiya, Y. Kohno and T. Hirai, *J. Org. Chem.*, 2008, **73**, 8571; (*b*) M. Zhu, M. Yuan, X. Liu, J. Xu, J. Lv, C. Huang, H. Liu, Y. Li, S. Wang and D. Zhu, *Org. Lett.*, 2008, **10**, 1481; (*c*) M. Yuan, W. Zhou, X. Liu, M. Zhu, J. Li, X. Yin, H. Zheng, Z. Zuo, C. Ouyang, H. Liu, Y. Li and D. Zhu, *J. Org. Chem.*, 2008, **73**, 5008.

